



# TRPC proteins contribute to development of diabetic retinopathy and regulate glyoxalase 1 activity and methylglyoxal accumulation

Robin Sachdeva<sup>1,9</sup>, Andrea Schlotterer<sup>2,9</sup>, Dagmar Schumacher<sup>1,9</sup>, Christin Matka<sup>1,9</sup>, Ilka Mathar<sup>1</sup>, Nadine Dietrich<sup>2</sup>, Rebekka Medert<sup>1</sup>, Ulrich Kriebs<sup>1</sup>, Jihong Lin<sup>2</sup>, Peter Nawroth<sup>3,4,5,6</sup>, Lutz Birnbaumer<sup>7,8</sup>, Thomas Fleming<sup>3,4</sup>, Hans-Peter Hammes<sup>2</sup>, Marc Freichel<sup>1,\*</sup>

## ABSTRACT

**Objective:** Diabetic retinopathy (DR) is induced by an accumulation of reactive metabolites such as ROS, RNS, and RCS species, which were reported to modulate the activity of cation channels of the TRPC family. In this study, we use *Trpc1/4/5/6*<sup>-/-</sup> compound knockout mice to analyze the contribution of these TRPC proteins to diabetic retinopathy.

**Methods:** We used Nanostring- and qPCR-based analysis to determine mRNA levels of TRPC channels in control and diabetic retinae and retinal cell types. Chronic hyperglycemia was induced by Streptozotocin (STZ) treatment. To assess the development of diabetic retinopathy, vaso-regression, pericyte loss, and thickness of individual retinal layers were analyzed. Plasma and cellular methylglyoxal (MG) levels, as well as Glyoxalase 1 (GLO1) enzyme activity and protein expression, were measured in WT and *Trpc1/4/5/6*<sup>-/-</sup> cells or tissues. MG-evoked toxicity in cells of both genotypes was compared by MTT assay.

**Results:** We find that *Trpc1/4/5/6*<sup>-/-</sup> mice are protected from hyperglycemia-evoked vasoregression determined by the formation of acellular capillaries and pericyte drop-out. In addition, *Trpc1/4/5/6*<sup>-/-</sup> mice are resistant to the STZ-induced reduction in retinal layer thickness. The RCS metabolite methylglyoxal, which represents a key mediator for the development of diabetic retinopathy, was significantly reduced in plasma and red blood cells (RBCs) of STZ-treated *Trpc1/4/5/6*<sup>-/-</sup> mice compared to controls. GLO1 is the major MG detoxifying enzyme, and its activity and protein expression were significantly elevated in *Trpc1/4/5/6*-deficient cells, which led to significantly increased resistance to MG toxicity. GLO1 activity was also increased in retinal extracts from *Trpc1/4/5/6*<sup>-/-</sup> mice. The TRPCs investigated here are expressed at different levels in endothelial and glial cells of the retina.

**Conclusion:** The protective phenotype in diabetic retinopathy observed in *Trpc1/4/5/6*<sup>-/-</sup> mice is suggestive of a predominant action of TRPCs in Müller cells and microglia because of their central position in the retention of a proper homeostasis of the neurovascular unit.

© 2018 The Authors. Published by Elsevier GmbH. This is an open access article under the CC BY-NC-ND license (<http://creativecommons.org/licenses/by-nc-nd/4.0/>).

**Keywords** Diabetic retinopathy; Reactive metabolites; TRPC cation channels; Methylglyoxal; Vasoregression; Glyoxalase1

## 1. INTRODUCTION

Reactive metabolites (RM), which accumulate under hyperglycemia, include reactive carbonyl (RCS), oxygen (ROS), and nitrogen (RNS) species, all of which contribute to the progression of diabetic long-term complications [1]. Such metabolites can impair the function of multiple cell types involved in diabetes-associated organ dysfunction leading to neuropathies and vasculopathies [1,2]. RM evoke post-translational

modifications of numerous signaling molecules. Several types of cation channels have been identified as target molecules of such metabolites accumulating under hyperglycemia. The dicarbonyl methylglyoxal binds to Na<sub>v</sub>1.8 sodium channels to reduce inactivation and increase the excitability of nociceptive neurons [3]. Extracellular application of MG also activates TRPA1 channels by reversible binding to cysteine residues following permeation of the cell membrane. MG-mediated activation of TRPA1 leads to a rise in the intracellular

<sup>1</sup>Institute of Pharmacology, Heidelberg University, Im Neuenheimer Feld 366, 69120 Heidelberg, Germany <sup>2</sup>Vth Department of Medicine, Medical Faculty Mannheim, Heidelberg University, Mannheim, Germany <sup>3</sup>Department of Medicine I and Clinical Chemistry, University Hospital Heidelberg, Germany <sup>4</sup>German Center for Diabetes Research (DZD), Germany <sup>5</sup>Institute for Diabetes and Cancer IDC Helmholtz Center Munich, Neuherberg, Germany <sup>6</sup>Joint Heidelberg-IDC Translational Diabetes Program, Dept. of Medicine I, Heidelberg University Hospital, Heidelberg, Germany <sup>7</sup>Neurobiology Laboratory, National Institute of Environmental Health Sciences, North Carolina, USA <sup>8</sup>Institute for Biomedical Research (BIOMED), School of Medical sciences, Catholic University of Argentina, Buenos Aires, Argentina

<sup>9</sup> Contributed equally.

\*Corresponding author. Fax: +49 6221 54 8644. E-mail: [marc.freichel@pharma.uni-heidelberg.de](mailto:marc.freichel@pharma.uni-heidelberg.de) (M. Freichel).

**Abbreviations:** DR, Diabetic Retinopathy; GLO1, Glyoxalase 1; GSH, Glutathione; GSSG, Glutathione disulfide; HTA, Hemithioacetal; MEF, Mouse Embryonic Fibroblast; MG, Methylglyoxal; NO, Nitric oxide; RCS, Reactive carbonyl species; RNS, Reactive nitrogen species; ROS, Reactive oxygen species; STZ, Streptozotocin; TRPC, Transient Receptor Potential Canonical

Received September 1, 2017 • Revision received December 18, 2017 • Accepted January 2, 2018 • Available online 5 January 2018

<https://doi.org/10.1016/j.molmet.2018.01.003>

calcium concentration and subsequent release of Calcitonin Gene-related Peptide (CGRP) [4]. TRPA1 mediates MG-evoked acute pain sensation [5], but the causal contribution of TRPA1 to long-term complications is not established. Other diabetes-associated reactive metabolites, such as ROS and RNS, also significantly modulate the activity of cation channels of the TRP family including TRPC channels [6,7]. TRPC channels (TRPC1–TRPC7) are mammalian homologs of *trp* channels, originally discovered in *Drosophila* photoreceptor cells. Structurally, these channels have six transmembrane domains, and the pore is formed by transmembrane domain 5 and 6. Based upon the structural homology, the TRPC family can be divided into three subgroups, TRPC1/TRPC4/TRPC5, TRPC3/TRPC6/TRPC7, and TRPC2. FRET based assays and immunoprecipitations, using synaptosomal protein fractions from cerebellum or cortex, have provided evidence for the interaction of TRPC1, TRPC4, and TRPC5, suggesting that they form heteromeric channels [8,9]. Recently, the formation of heteromeric channels by TRPC1, TRPC4, and TRPC5 was demonstrated using quantitative high-resolution mass spectrometry on affinity-purifications (APs) from total brain and in hippocampus neurons using isoform specific antibodies [10]. In the embryonic brain, TRPC1 and TRPC4 could also be co-immunoprecipitated with TRPC6 [11]. The cation channels formed by TRPC proteins are permeant for  $Ca^{2+}$  and  $Na^{+}$  under physiological conditions and are activated in response to activation of phospholipase C-coupled receptors but also by various reactive metabolites accumulating under diabetic conditions [12,13]. For TRPC5, it has been shown that nitric oxide (NO) donors lead to S-nitrosylation of cysteine residues in the channel pore, evoking an increased open probability of the channel [14]. TRPC5 channel activity was also increased by application of the reduced form of thioredoxin [15] or by application of oxidised glutathione (GSSG) [16]. TRPC1 and TRPC4 modulate the sensitivity of TRPC5 channels towards RNS and ROS [14]. TRPC3, TRPC4, and TRPC6 were also found to be redox-sensitive channels, and their expression and activity were reported to be modulated by ROS species [17,18].

Numerous studies have investigated the differential regulation of members of the TRPC subfamily in experimental models of diabetes, including the streptozotocin (STZ) model, Zucker obese rat, Goto-Kakizaki rats, and *db/db* mice, as well as in human cells cultured under hyperglycemic conditions. However, depending on the study and the model system used, contradictory findings have been reported with respect to the transcription and expression of the TRPCs [19]. So far, the functional relevance of TRPC cation channels in diabetic complications was primarily analyzed at the cellular level, e.g. in cells contributing to microangiopathy and nephropathy such as cultured vascular smooth muscle cells, platelets or mesangial cells [19]. The relevance of TRPCs for diabetic complications has not been studied in complex disease models, in part, due to the lack of specific antagonists for individual TRPC channels, as well as the limitations of knock-down approaches for long-term studies *in vivo*.

To date, diabetic retinopathy is a prevalent complication, and is expected to increase in magnitude, given the global epidemic of type 2 diabetes, and the lack of a specific systemic treatment beyond glucose control. Treatments such as laser photocoagulation and intravitreal injections of anti-proliferative or anti-inflammatory agents aim at late disease stages, are invasive by nature, and have significant side effects. Diabetic retinopathy (DR) in rodents and humans affects almost all cell types and culminates in impaired function and structure from the point of inception. The initial vascular phenotype is vasoregression, i.e. the loss of pericytes and endothelial cells. Neurodegeneration leading to a reduction of retinal thickness can occur as a consequence of progressive retinal capillary drop-out [20] but also as an independent

process involving progressive cell death by apoptosis. In this process, accumulation of reactive metabolites and MG can play an important role [20,21].

In this study, the causal contribution of four TRPC proteins, TRPC1, TRPC4, TRPC5, and TRPC6, was investigated with respect to their role in DR by comparing *Trpc1/4/5/6*<sup>-/-</sup> (TRPC QKO) mice to wild-type controls in the STZ-induced model of diabetes.

## 2. METHODS

### 2.1. Mice

To analyze the mRNA expression level of TRPCs by Nanostring, we used wild-type and *Ins2*<sup>Akita</sup> mice with C57BL/6J background as a model for type 1 diabetes [22]. The quadruple *Trpc* knockout mouse line *Trpc1/4/5/6*<sup>-/-</sup> was generated by intercrossing mice of the four mouse lines *Trpc1*<sup>-/-</sup> [23], *Trpc4*<sup>-/-</sup> [24], *Trpc5*<sup>-/-</sup> [25], and *Trpc6*<sup>-/-</sup> [26] mice. The *Trpc1/4/5/6*<sup>-/-</sup> mice had a mixed C57Bl6-129SvJ genetic background, and age and sex matched first generation (F1) offspring of C57Bl6/N and 129SvJ matings were used as controls. *Trpc1/4/5/6*<sup>-/-</sup> mice were routinely genotyped using primers specific for the corresponding *Trpc*-deficient alleles as described before [23–26]. Both mouse lines were bred and maintained at our university's Specific Pathogen Free (SPF) central animal facility. We used 8–12 weeks old male mice and treated them with STZ (Sigma–Aldrich, Taufkirchen, Germany) as described previously [3]. Briefly, mice received one STZ injection/day i.p. (60 mg/kg) for five days, and blood glucose levels were maintained in the range of 300–500 mg/dl by insulin glargine treatment twice weekly according to blood glucose levels (Accu-Chek Aviva, Roche, Mannheim, Germany). Glycated hemoglobin (HbA<sub>1c</sub>) was determined by cation-exchange chromatography on a PolyCAT A column [27]. Mice were kept in standard 12 h light/dark cycle and provided free access to standard chow diet and water. Markers for retinopathy, neurodegeneration, and methylglyoxal measurement were analyzed 30 weeks after the development of hyperglycemia. All animal experiments were conducted in accordance with the relevant guidelines by the EU Directive 2010/63/EU and approved by the local Animal Care and Use Committee at the regional authority in Karlsruhe, Germany.

### 2.2. Analysis of TRPC expression in retina

Total RNA was extracted from retinæ of 8-month-old *Ins2*<sup>Akita</sup> mice and nondiabetic control mice using TRIzol method (Thermo Fisher, Germany). RNA concentrations were measured using spectrophotometer (Infinite 200 PRO Nanoquant, TECAN, Austria) and microfluidic analysis (Bioanalyzer 2100, Agilent Technologies, USA). Analysis of the transcripts was done by NCounter Nanostring technology in a three-step method described by Geiss et al. [28]. Briefly, in the first step, two probes, the reporter and the capture probe, hybridize directly to the target molecule in solution. Then, the target–probe complexes are immobilized on the imaging surface of the nCounter Cartridge by binding to the capture probe. Finally, the sample cartridges are scanned by an automated fluorescence microscope, and molecular barcodes (fluorophores contained in the reporter probe) for each specific target are counted. For expression analysis by NCounter NanoString technology, 1 µg total RNA was hybridized (four biological replicates, RIN > 8.3) with a Nanostring Gene Expression CodeSet and analyzed using the nCounter Digital Analyzer (Nanostring Technologies, Seattle, USA). Background correction was performed, and normalization was applied using 5 different reference genes (*Hprt1*, *Tbp*, *Ubc*, *Gapdh*, *Actb*). *Trpc* specific DNA sequences used are listed in Supplementary Table 1.

### 2.3. Quantification of vasoregression and pericyte loss

Quantitative retinal morphometry was performed on retinal digest preparations to evaluate numbers of acellular capillaries (ACs/mm<sup>2</sup> retinal area) and pericytes (pericytes/mm<sup>2</sup> capillary area), according to published methods [29]. Briefly, after enucleation, eyes were fixed in 4% formalin for two days at room temperature. Retinae were isolated from the eyeball by opening it from the ora serrate. Isolated retinae were digested with 3% trypsin at 37 °C until the photoreceptor layer, and other retinal layers were digested, leaving behind the vasculature that can be seen under the low magnification microscope. To visualize the retinal morphology and morphometry, PAS staining was performed on the digested retinae. Microscopic quantification of acellular capillaries was done using the Cell-F software (Olympus opticals, Hamburg, Germany). Acellular capillaries were analyzed in ten randomly selected areas of the central retina (the area around the optic nerve). The total number of acellular capillaries was calculated to the total retina area. The total number of pericytes was analyzed in the ten randomly selected fields in the central retina under 400x magnification.

### 2.4. Expression analysis in cell lines and retinae using qPCR

RNA isolation was performed using the RNeasy Mini kit (Qiagen) according to manufacturer's protocol for cells, including on-column DNase digest. For human Müller cells, cells were derived from one retina, for rat brain microglia from one Sprague Dawley rat, for Bovine Retinal Endothelial cells (BRECs) from 15 bovine retinae. cDNA synthesis was carried out using the SensiFAST cDNA synthesis kit (Bioline) according to manufacturer's recommendations. Primers were designed with the online tool provided by Roche ([https://lifescience.roche.com/en\\_de/brands/universal-probe-library.html](https://lifescience.roche.com/en_de/brands/universal-probe-library.html)) and the best primer pair for each target out of 2–3 was chosen from an initial qPCR screen. Quantitative expression analysis was performed using the Universal Probe system (Roche) with the corresponding FastStart Essential DNA Probes Master (Roche) on a LightCycler 96 Instrument (Roche, Mannheim, Germany). Relative expression levels were obtained by normalizing to H3F3A, AIP and CXXC1 expression levels. Primer sequences can be found in the [Supplementary Tables 2–4](#).

### 2.5. Retinal thickness and nuclei count

Analyzes of thickness and number of cells in retinal nuclear layers were performed as described before [30]. Briefly, 3 µm thick Periodic Acid Schiff's (PAS)- and hematoxylin-stained paraffin sections were used, and areas near the optic nerve were selected for measurements of the central retina using a microscope (Olympus, Hamburg, Germany) equipped with an analysis program (Olympus, Cell-F, Hamburg, Germany). The thickness of the entire retina and all retinal layers is expressed in µm. The number of cells in the ganglion cell layer is expressed per 250 µm of retinal length, the inner nuclear layer per 100 µm of retinal length and the outer nuclear layer per 50 µm of retinal length.

### 2.6. Methylglyoxal measurement in RBCs and plasma

The concentration of methylglyoxal in EDTA plasma and isolated RBCs was determined by derivatization with 1,2-diamino-4,5-dimethoxybenzene, according to the method described by McLellan [31].

### 2.7. Glyoxalase 1 activity

GLO1 activity was determined spectrophotometrically as described previously [32]. Briefly, the initial rate of change in absorbance at 235 nm, caused by the formation of S-D-lactoylglutathione by GLO1, is monitored. The assay mixture contained 2 mmol/L MG and 2 mmol/L

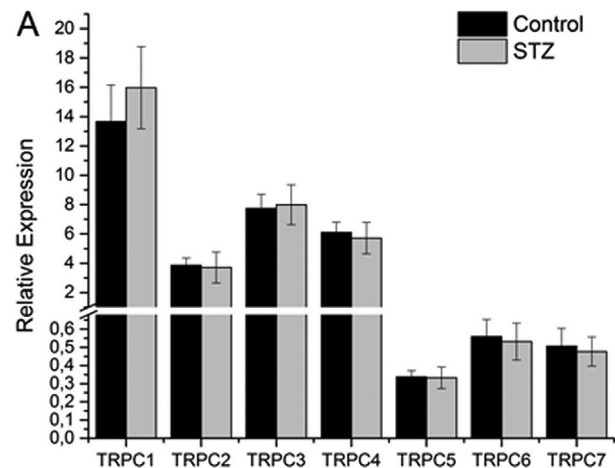


**Figure 1:** TRPC mRNA expression in Retina by qPCR. (A) RNA was extracted from retina of wild type mice 30 weeks after STZ or Citrate treatment. Absolute mRNA expression level of *Trpc* transcripts were normalized to expression level of house-keeping genes [ $n = 4$  (8 retinae) for WT citrate and  $n = 5$  (10 retinae) WT STZ samples].

GSH in sodium phosphate buffer (50 mmol/L, pH 6.6, 37 °C) and was incubated for 10 min to guarantee the complete formation of hemithioacetal (HTA). After the addition of the cytosolic protein fraction (5 µg/10 µL protein), the change in absorbance at 235 nm was monitored for 10 min. The activity of GLO1 is expressed in units (U), where 1 U is the amount of GLO1 which catalyzes the formation of 1 µmol/L of S-D-lactoylglutathione per minute.

### 2.8. Glyoxalase 1 protein expression

MEFs cytoplasmic extracts were used for GLO1 protein expression analysis using western blot. Samples were loaded on a precast 4–12% gel (Invitrogen, Germany) and run at 80 V for 15 min and after that at 130 V for more than 1 h until the dye front reached the bottom of the gel. Samples were blotted onto a nitrocellulose membrane using Bis-Tris blotting buffer containing 20% methanol. Blotting was done at 9 V for 1 h. After blotting, the membrane was blocked with 5% milk powder in 1x TBS-T. Blocking was followed by brief washing with 1x TBS-T, and then, the membrane was incubated in the primary GLO1 antibody (1:1000 diluted) (Abcam, UK) 12–15 h or overnight. The next day, the membrane was washed briefly with 1x TBS-T and then incubated for more than 2 h with an anti-rabbit secondary antibody (1:50000 diluted) (GE Healthcare, UK). After washing briefly with 1x TBS-T, protein bands were detected by ECL chemiluminescence. Densitometric analysis was done to determine the intensity of immunostainings using Image J software. The signal intensity obtained by the anti-GLO1 antibody was normalized to the signal intensity obtained by anti- $\alpha$ -Tubulin staining.

### 2.9. MTT assay

MEFs were seeded in 96 well-plates at a density of 25,000 cells per well and incubated overnight at 37 °C (5% CO<sub>2</sub>). The next day, cells were washed with PBS and then incubated with MG at the concentration indicated for 48 h. After that, 50 µL of MTT solution (2 mg/mL in H<sub>2</sub>O) was applied, and cells were incubated for 3 h. Subsequently, the medium was removed, and cells were lysed with 200 µL of DMSO. To dissolve the formazan crystals completely, the plate was incubated for another hour at room temperature, and then absorbance was measured at 590 nm with 620 nm as reference wavelength. Cell viability was calculated by normalizing the absorbance values for

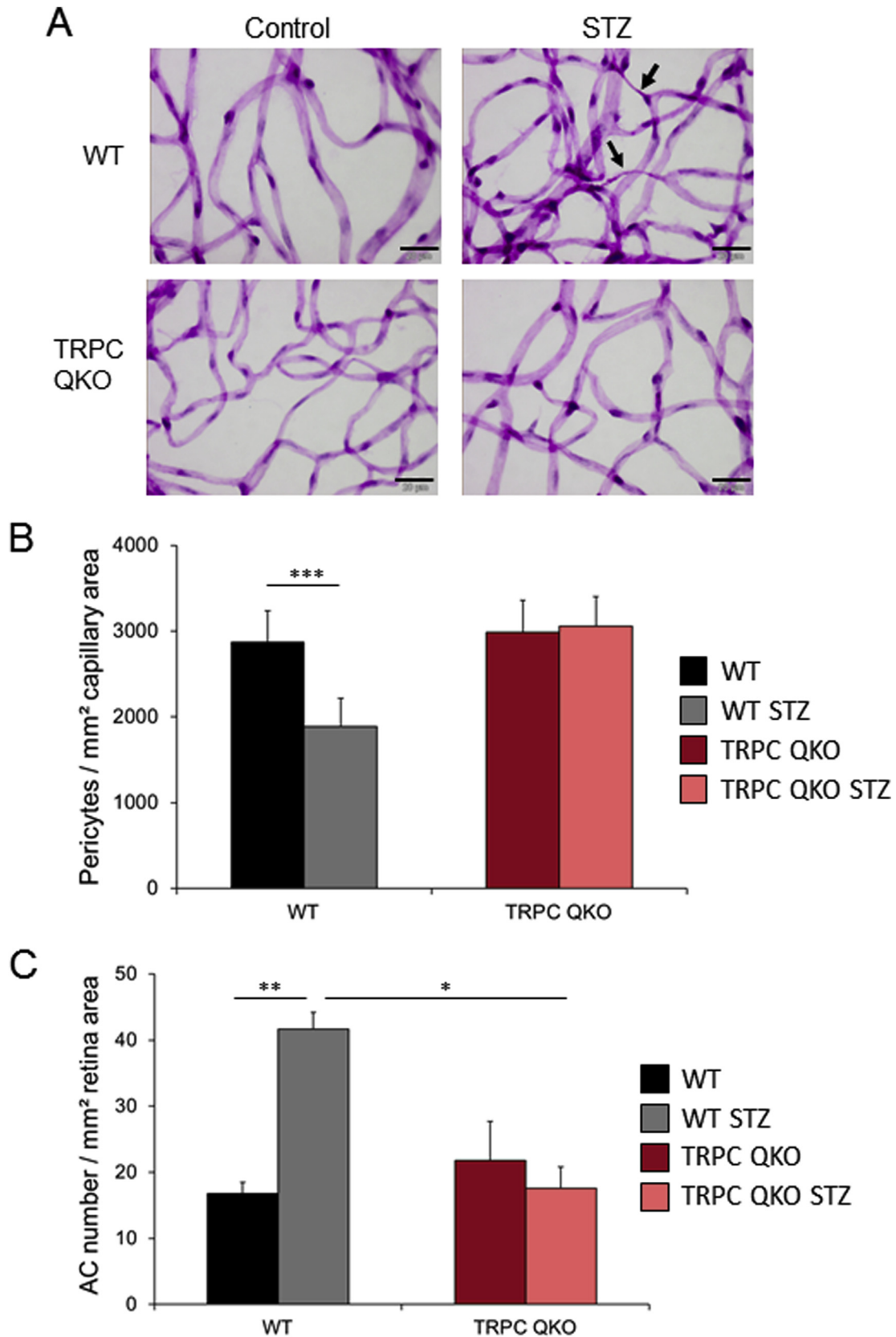


**Figure 2: Vasoregression and pericyte loss in diabetic retinae.** (A) Representative images of PAS-stained retinal digest preparations. Acellular capillaries (AC) are marked with black arrows, scale bar represents 20  $\mu\text{m}$ . (B) The number of pericytes per  $\text{mm}^2$  of the capillary area was calculated from ten random selected fields of the circular area around the optic nerve. (C) The number of acellular capillaries per  $\text{mm}^2$  of retina tissue was also analyzed in ten random selected fields of the circular area around the optic nerve. The number of animals analyzed for both acellular capillaries and pericyte loss was  $n = 5$  in WT control,  $n = 6$  in WT STZ-treated,  $n = 6$  in *Tpc1/4/5/6*<sup>-/-</sup> mice (TRPC QKO) control,  $n = 5$  in TRPC QKO STZ-treated, \*\*\* $p < 0.001$ .

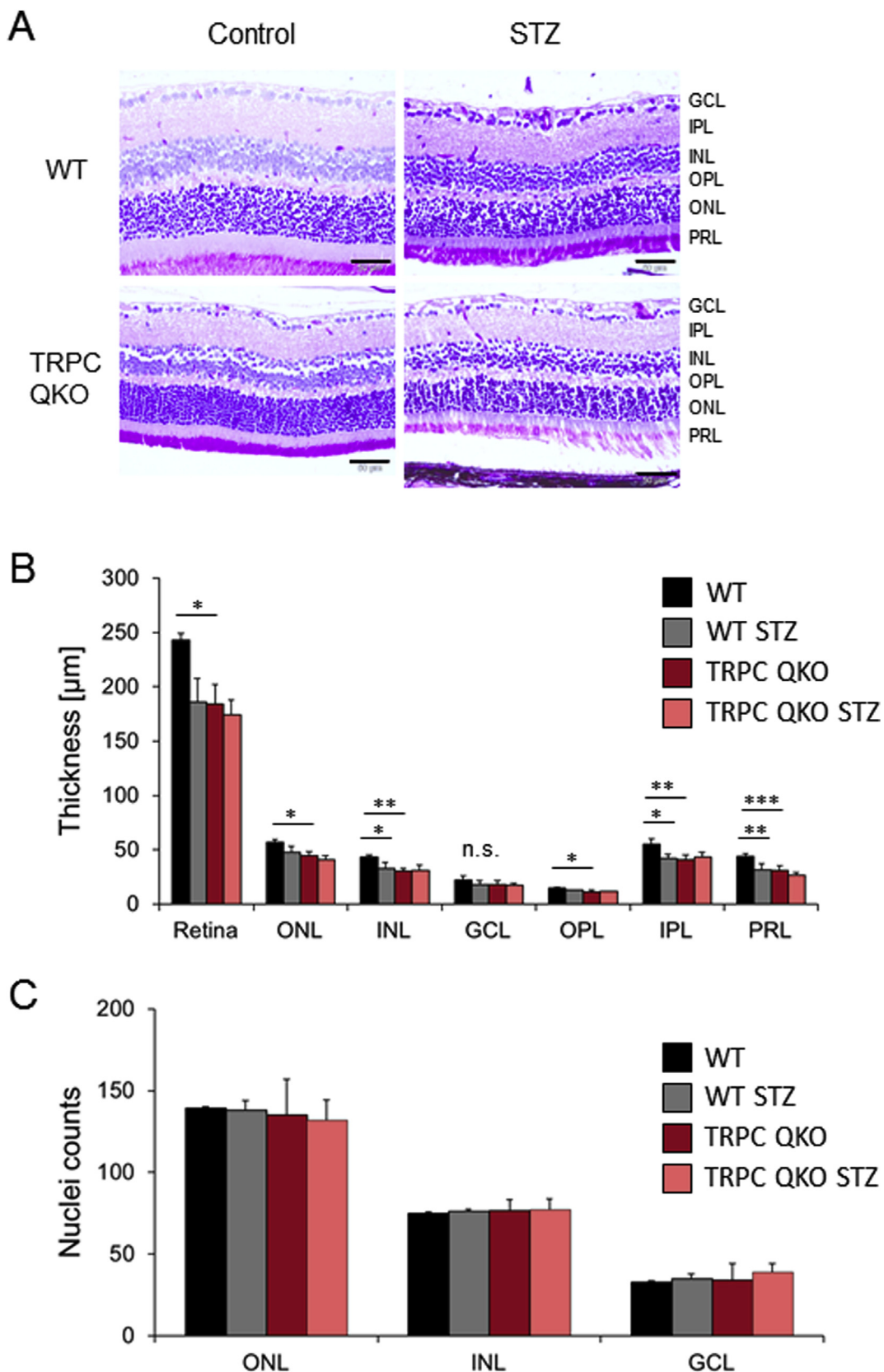


**Figure 3: Analysis of central retinal thickness.** (A) Representative images of retinal layers for all experimental groups, scale bar represents 50  $\mu\text{m}$ . (B) Total retinal thickness and thickness of each retinal layer at the center were measured in diabetic WT and *Trpc1/4/5/6*<sup>-/-</sup> (TRPC QKO) mice and in the respective non-diabetic controls. ONL: Outer nuclear layer, INL: Inner nuclear layer, GCL: Ganglionic cell layer, OPL: Outer plexiform layer, IPL: Inner plexiform layer, PRL: Pigmented retinal layer. (n = 4 for WT and TRPC QKO diabetic and for the respective controls, \*p < 0.05, \*\*p < 0.01 and \*\*\*p < 0.001). (C) Analysis of number of nuclei in central retina in different retinal layers. A total number of nuclei in each retinal layer was counted in diabetic WT and TRPC QKO mice and also in their non-diabetic controls (n = 4 for WT and TRPC QKO diabetic and non-diabetic controls).

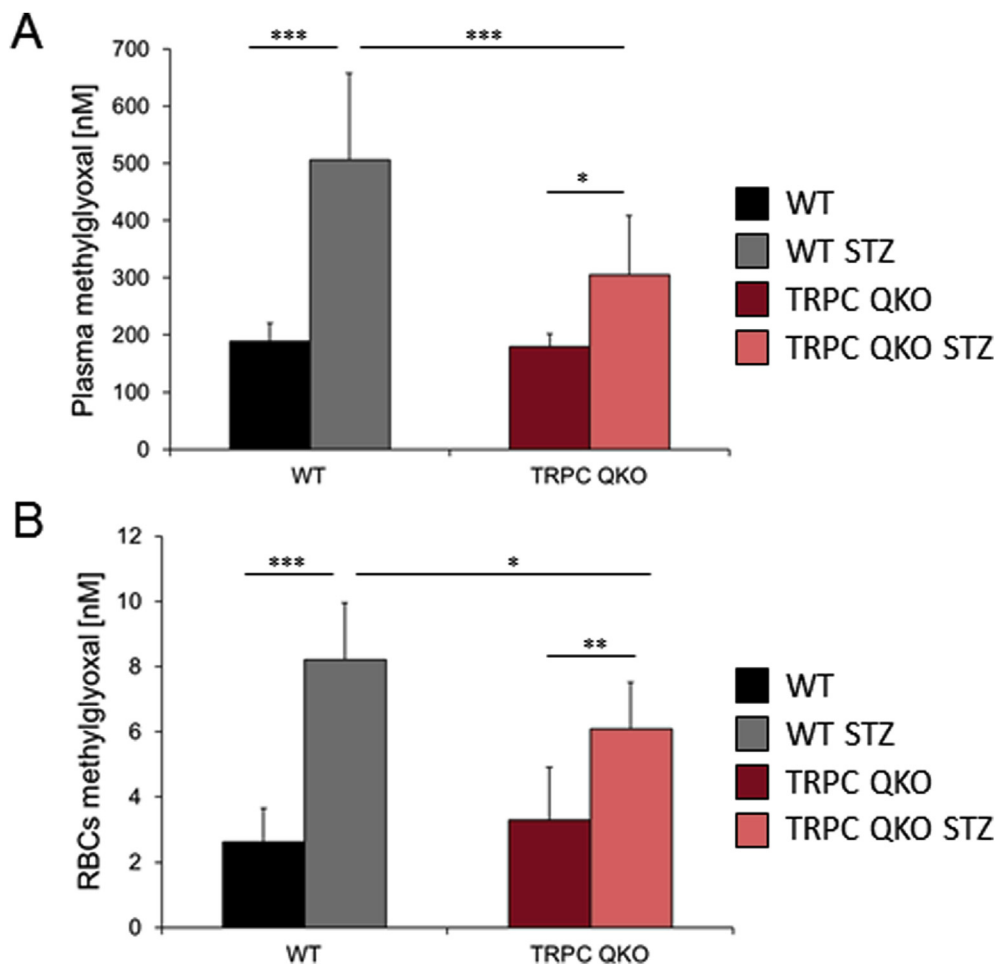


**Figure 4: Methylglyoxal levels in plasma and red blood cells.** (A) and (B) 30 weeks after STZ treatment, methylglyoxal levels were measured in plasma (a) and red blood cells (RBCs) (b) of diabetic WT and *Trpc1/4/5/6*<sup>-/-</sup> (TRPC QKO) mice and also in the non-diabetic control groups with a HPLC-based assay. MG levels were normalized to total haemoglobin and protein content in RBCs and plasma, respectively (n = 10 mice for nondiabetic WT controls, n = 14 diabetic WT mice, n = 11 mice for non-diabetic TRPC QKO controls, n = 7 diabetic TRPC QKO mice, \*p < 0.05, \*\*p < 0.01 and \*\*\*p < 0.001).

treated cells with the absorbance values of non-treated cells and expressed in percent.

#### 2.10. Isolation of mouse embryonic fibroblast (MEF) cells

Primary mouse embryonic fibroblast (MEF) cells were isolated from E13.5 wild-type control and *Trpc1/4/5/6*<sup>-/-</sup> embryos, respectively, as described previously [24,33]. Cells were propagated in DMEM high glucose medium (Invitrogen, Germany) and used at passage 2 for enzyme activity, western blot, and MTT assay.

#### 2.11. Statistical analysis

Results are shown as mean ± SD, unless stated otherwise. Statistical significance for Figures 2–4 and Supplementary Figure 1 was determined by two-way ANOVA (*Tukey Test*) whilst two-tailed unpaired Student's *t*-test was used in all other figures. Differences with p < 0.05 were considered statistically significant. Significances are depicted as \* p < 0.05, \*\* p < 0.01, and \*\*\* p < 0.001.

### 3. RESULTS

#### 3.1. TRPC channels are abundantly expressed in retina

The expression pattern of *Trpc* genes in the retina under diabetic conditions was assessed using qPCR-based RNA analysis from citrate

and STZ-treated wild type mice (Figure 1). Several TRPC channels were found to be abundantly expressed in the mouse retina. Transcripts of *Trpc1*, *Trpc2* (a pseudogene in humans), *Trpc3*, and *Trpc4* showed the highest relative expression, but *Trpc5*, *Trpc6*, and *Trpc7* were also identified. In addition, we studied *Trpc* transcript abundance using a Nanostring-based RNA analysis in retinae of 32-week old control and *Ins2*<sup>Akita</sup> mice, which spontaneously develop diabetes due to a missense mutation in the insulin 2 gene. Also, here, most TRPC channels were found to be abundantly expressed. Specifically, *Trpc1* mRNA was detected at very high levels, followed by *Trpc3*, *Trpc4*, and *Trpc6* transcript levels in control as well as in the diabetic retinae. Expression of TRPC5 was also detectable. Notably, *Trpc6* transcript levels were significantly higher in the retina of *Ins2*<sup>Akita</sup> mice compared to controls indicating an upregulation of TRPC6 transcripts under diabetic conditions (Supplementary Figure 2A).

#### 3.2. *Trpc1/4/5/6* quadruple knockout mice are protected from experimental diabetic retinopathy

To study the contribution of several TRPCs simultaneously in the diabetic condition, the *Trpc* compound knockout mouse line *Trpc1/4/5/6*<sup>-/-</sup> was used. In these mice, cation channels formed by TRPC1-, TRPC4-, TRPC5- and/or TRPC6 which are all subject to modulation by reactive metabolites have been inactivated. After 30 weeks of constant

hyperglycemia, mice were killed and retinopathy was assessed. In STZ-diabetic wild-type mice, we observed a marked decrease in the number of pericytes compared to non-diabetic controls. In contrast, diabetic *Trpc1/4/5/6*<sup>-/-</sup> mice were completely protected from pericyte loss (Figure 2B). Consecutively, the formation of acellular capillaries as a measure of both, pericyte and endothelial cell loss, was increased in hyperglycemic control mice compared to the normoglycemic condition (Figure 2A,C), but in diabetic *Trpc1/4/5/6*<sup>-/-</sup> mice, formation of acellular capillaries was completely absent (Figure 2A,C). These results suggest that TRPC1-, TRPC4-, TRPC5-, and TRPC6-containing cation channels contribute to diabetic vasoregression.

### 3.3. Diabetes-evoked retinal neurodegeneration is reduced in *Trpc1/4/5/6* quadruple knockout mice

We also aimed to analyze whether TRPC1/4/5/6 proteins play a role in neurodegeneration in the retina induced by the metabolic changes under chronic hyperglycemia. STZ-induced hyperglycemia reduced the overall retinal thickness, composed of the thickness of individual retinal layers measured in the center of the retina. Specifically, the outer nuclear layer (ONL), the inner nuclear layer (INL), the outer plexiform layer (OPL), the inner plexiform layer (IPL) and the pigmented retinal layer (PRL) were reduced in thickness under diabetic conditions in wild-type mice. Only the ganglion cell layer (GCL) was unaffected by diabetes (Figure 3A,B). In contrast, there was no hyperglycemia-induced change in the thickness in any retinal cell layer in *Trpc1/4/5/6*<sup>-/-</sup> mice. The number of nuclei in the retina of both wild-type and *Trpc1/4/5/6*<sup>-/-</sup> mice was unchanged (Figure 3C).

### 3.4. TRPC channels are involved in the accumulation of reactive metabolites in tissues

To investigate the observed protection against the development of diabetic retinopathy in *Trpc1/4/5/6*<sup>-/-</sup> mice, we asked whether *Trpc1/4/5/6*<sup>-/-</sup> mice were exposed to a comparable glucose-dependent metabolic stress as wild-type controls, even though the HbA<sub>1c</sub> levels were not different between the two genotypes (Supplementary Figure 1A). An increase in the levels of the reactive metabolite methylglyoxal is known to mediate the development of diabetic retinopathy and was found in plasma samples of STZ-diabetic wild-type mice. However, in STZ-diabetic *Trpc1/4/5/6*<sup>-/-</sup> mice, the rise of MG plasma levels was significantly reduced compared to the STZ-treated wild-type group (Figure 4A). To examine whether the reduced extracellular accumulation of MG is also observed inside the cell, MG content in red blood cells (RBCs) was analyzed, and results show that the STZ-induced increase in MG levels in wild-type RBCs was again significantly reduced in *Trpc1/4/5/6*<sup>-/-</sup> mice to a similar extent as in the plasma (Figure 4B). These results suggest that TRPC channels are involved in the accumulation of the major hyperglycemia-related reactive metabolite MG.

### 3.5. Increased Glyoxalase 1 activity and protein expression enhances MG tolerance in *Trpc1/4/5/6*<sup>-/-</sup> cells

As GLO1 is a key enzyme in the detoxification of MG, we measured GLO1 enzyme activity in MEFs derived from *Trpc1/4/5/6*<sup>-/-</sup> mice. We detected a significant increase in GLO1 activity in *Trpc1/4/5/6*<sup>-/-</sup> MEFs (Figure 5A), which was accompanied by an increased expression of the GLO1 protein (Figure 5B). We hypothesized that *Trpc1/4/5/6*<sup>-/-</sup> cells are more resistant towards MG due to this increase in GLO1 activity. To test this hypothesis, MTT-based viability assays were performed. We detected a right shift in the dose–response curve in *Trpc1/4/5/6*<sup>-/-</sup> MEFs (IC<sub>50</sub> 484 ± 108 μmol/L) as compared to wild-type controls (IC<sub>50</sub> 305 ± 31 μmol/L, Figure 5C). Accordingly, the

percentage of viable *Trpc1/4/5/6*<sup>-/-</sup> MEFs was significantly higher compared to wild-type controls at a MG concentration of 500 μmol/L, indicating that they can tolerate detrimental MG levels better than the wild-type controls (Figure 5C, insert).

### 3.6. Increased Glyoxalase 1 activity in the retina may confer protection against development of diabetic retinopathy in *Trpc1/4/5/6*<sup>-/-</sup> mice

The increased GLO1 activity detected in MEFs could be confirmed in vivo in the retinae isolated from *Trpc1/4/5/6*<sup>-/-</sup> mice (Figure 6A,B). To analyze the expression of TRPC channels in cell types relevant to the development of DR, we measured mRNA levels in primary human Müller cells, in primary rat brain microglia and bovine retinal endothelial cells via quantitative real-time PCR (qPCR). Predominant and very high expression of TRPC1 compared to reference genes was observed in human Müller cells (Figure 6C) with *Trpc4* and *Trpc5* mRNAs also being detected. In rat microglia (Figure 6D), *Trpc1* was also the major family member expressed in these cells, accompanied by low levels of *Trpc6* mRNA. In bovine retinal ECs (Figure 6E), *Trpc1*, *Trpc4*, and *Trpc5* transcripts were highly abundant and *Trpc2*, and *Trpc6* mRNAs were present at low levels. Thus, *Trpc1* is highly expressed in all cell types tested, and *Trpc4* and *Trpc5* are present in relevant amounts in Müller cells and retinal ECs.

## 4. DISCUSSION

In this study, we find that *Trpc1/4/5/6*<sup>-/-</sup> mice are protected from damage to the neurovascular unit and lack hyperglycemia-evoked vasoregression, a hallmark of DR, determined by the formation of acellular capillaries and pericyte drop-out. DR is accompanied by microangiopathic and neurodegenerative changes and cell death, which also leads to a reduction in overall thickness and thickness of the single retinal layers. However, the retinal layer thickness is unchanged by hyperglycemic conditions in *Trpc1/4/5/6*<sup>-/-</sup> mice in contrast to a marked reduction of layer thickness in hyperglycemic wild-types in all layers except the retinal ganglion cell layer.

Diabetic complications such as retinopathy are mediated by an accumulation of reactive metabolites that include ROS, RNS, and RCS species. TRPC channel function can be modulated by such metabolites, but so far, a causative contribution of TRPC channels to diabetic complications has not been shown. Despite similar levels of hyperglycemia, *Trpc1/4/5/6*<sup>-/-</sup> mice showed reduced accumulation of the reactive metabolite methylglyoxal in plasma and RBCs. MG has been shown to contribute to the pathology of DR [21]. GLO1 is considered as the major enzyme involved in the detoxification of MG, and we found an increase in GLO1 enzyme activity in MEFs derived from TRPC1/4/5/6-deficient mice and in retina lysates from these mice. GLO1 protein levels were also increased compared to wild-type mice. We found this increase in GLO1 activity to be sufficient to mediate significant protection from MG-evoked cellular toxicity. These results indicate that TRPC channels containing any of the four TRPC1/C4/C5/C6 proteins are involved in the regulation of GLO1 activity, and loss of these channels leads to an increase in GLO1 activity and MG detoxification which may confer protection from retinopathic changes in vivo.

As we used TRPC-deficient mice with ubiquitous deletion of these proteins, our approach did not allow to differentiate in which retinal cell type(s) these channel proteins contribute to the development of retinopathy. However, we identified abundant expression of TRPC1, C4, and C5 in bovine retinal endothelial cells, which form heteromeric channels in other cells such as hippocampal neurons [10]. Additionally, we found TRPC1 to be predominantly expressed in rat brain microglial

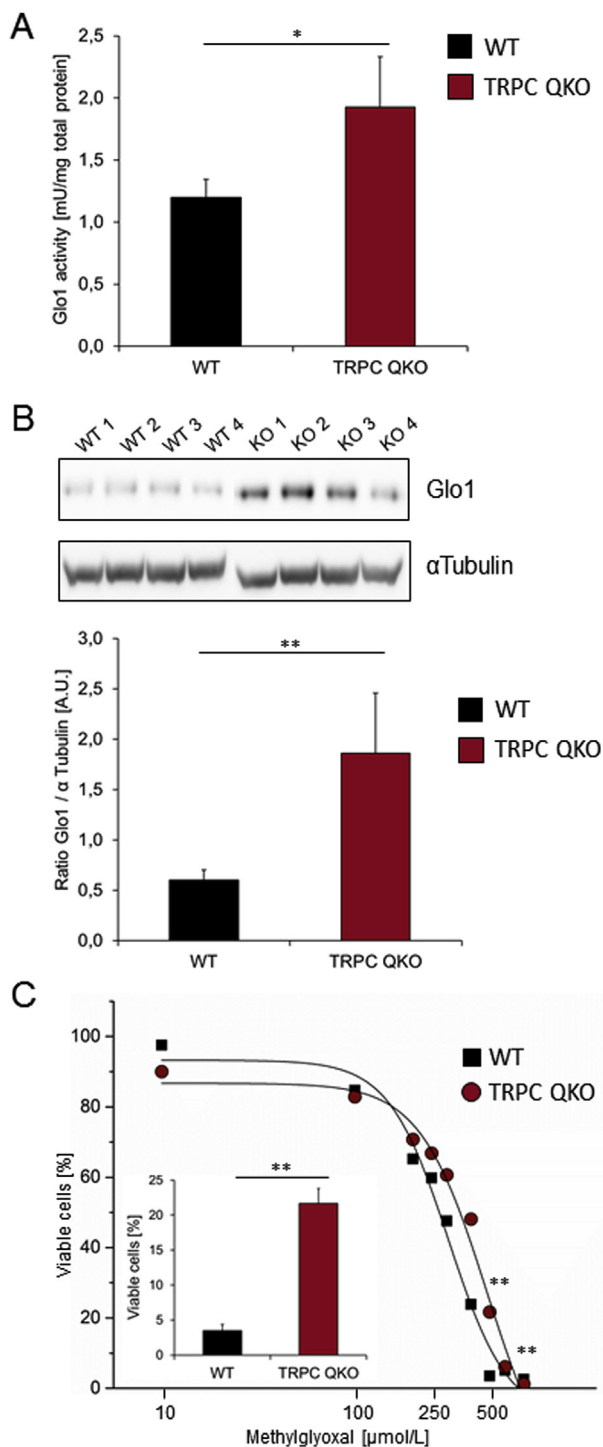


**Figure 5: Increased Glyoxalase 1 activity and protein expression enhance MG tolerance in *Trpc1/4/5/6*<sup>-/-</sup> cells.** (A) Cytoplasmic extracts of lysed mouse embryonic fibroblasts (MEFs) were used to determine glyoxalase 1 (GLO1) activity. The bar graph shows the averaged GLO1 activity from three independent wild-type and *Trpc1/4/5/6*<sup>-/-</sup> MEF preparations (\*p < 0.05). (B) Upper panel: GLO1 protein expression in MEFs was analyzed in cytoplasmic extracts from MEF cells. Immunoblot with samples of 4 independent wild-type (WT1-WT4) and *Trpc1/4/5/6*<sup>-/-</sup> KO1-KO4) MEF preparations using anti-GLO1 antibody are shown.  $\alpha$ -tubulin was used as loading control. Lower panel: Densitometric quantitative analysis of the western blot shown above. The bar graph shows the average GLO1 to  $\alpha$ -tubulin ratio of the 4 wild-type and TRPC QKO MEFs samples, respectively (\*\*p < 0.01). (C) Large panel: Dose response curve for MG-evoked cell toxicity in MEFs. MEFs were incubated with varying concentration of

cells with low levels of TRPC6, but protein expression in mouse retinal glia cells could not be shown so far because all anti-TRPC antibodies tested in retinal sections were not able to distinguish between wild-type and the corresponding TRPC knockout. A functional role of TRPCs is also conceivable in Müller cells since we find very high expression of *Trpc1* transcripts in primary human Müller cells, but functional studies investigating TRPC signaling are still lacking for this cell type. Although the exact mechanism(s) by which GLO1 is modulated through TRPC activity need(s) to be determined, it appears that Müller cells are central to the homeostasis of the neurovascular unit. For example, the receptor for advanced glycation end products, RAGE, is strongly expressed and upregulated in Müller glia and microglia under diabetic conditions, and in mice with a deletion of RAGE, protection from vasoregression is observed [34]. Moreover, when the reactive metabolite methylglyoxal is reduced by treating diabetic rats with a DPP-4 inhibitor, both vasoregression and neurodegeneration are reduced [30]. On the other hand, all four of the TRPC proteins were previously shown to mediate calcium entry in endothelial cells [24,35–38]. An exaggerated rise in  $[Ca^{2+}]_i$ , that could be triggered by reactive metabolites including ROS or RNS following hypoxia, leads to apoptotic death [39] and eventually to the development of acellular capillaries, which is blunted in the absence of these channel proteins. The underlying processes of  $Ca^{2+}$ -overload-mediated toxicity may include over-activation of several types of enzymes, e.g. proteases of the calpain family, the phosphatase calcineurin, NO synthases and endonucleases leading to DNA fragmentation. Activation of calcineurin was shown to be downstream of signaling by TRPCs channels including TRPC1/C4/C6 [40]. Calpain can cleave and activate TRPC5 and may thus further aggravate this process [41]. In analogy, similar mechanisms could be envisaged in pericytes to evoke  $Ca^{2+}$ -dependent pericyte loss under diabetic conditions. In contrast to endothelial cells, pericytes are electrically excitable cells which have voltage-gated  $Ca^{2+}$  channels (VGCC) in addition to agonist-evoked  $Ca^{2+}$  entry pathways triggered by GPCR agonists such as ET-1, Ang II or ATP [42,43], which might be conveyed by TRPC channels in analogy to vascular smooth muscle cells [44]. Similarly as in astrocytes [45], in which TRPC channels were reported to coordinate ion signaling, and in Müller cells, a significant contribution of TRPC channels to such pathological processes has also not been demonstrated in pericytes, but ATP-evoked pericyte death was shown to be mediated via  $P_2X_7$  purinoreceptors [42].

The exact entities of TRPC complexes that are thought to consist of heteromers or homomers of individual TRPC proteins could not be pinpointed in the retina in our study. TRPC proteins can interact with STIM1 proteins [46], which contain redox-sensing cysteine residues [47], but redox-mediated activation of STIM proteins could also engage cation entry via channels consisting of Orai proteins [47,48]. Under diabetic conditions, TRPC5-containing channels could be involved in redox signaling beyond their stimulation by RNS species [6,7,14]. Very recently, it was reported that the  $H_2O_2$ -evoked ROS production, as well as premature senescence, was reduced in primary endothelial cells of TRPC5-deficient mice [49], suggesting that TRPC5 channels are not only a target of these metabolites but also a determinant of its

MG for 48 h. The percentage of living cells was determined by MTT assay. Closed black squares represent the average of viable wild-type MEFs and the closed white circles the percentage of viable *Trpc1/4/5/6*<sup>-/-</sup> MEFs at the given MG concentrations. Three independent wild-type and *Trpc1/4/5/6*<sup>-/-</sup> MEF preparations were analyzed (\*\*p < 0.01). The insert shows a bar graph of the mean values from the MTT assay for the three MEF preparations per genotype after treatment with 500  $\mu$ mol/L MG (\*\*p < 0.01, error bars: SEM).

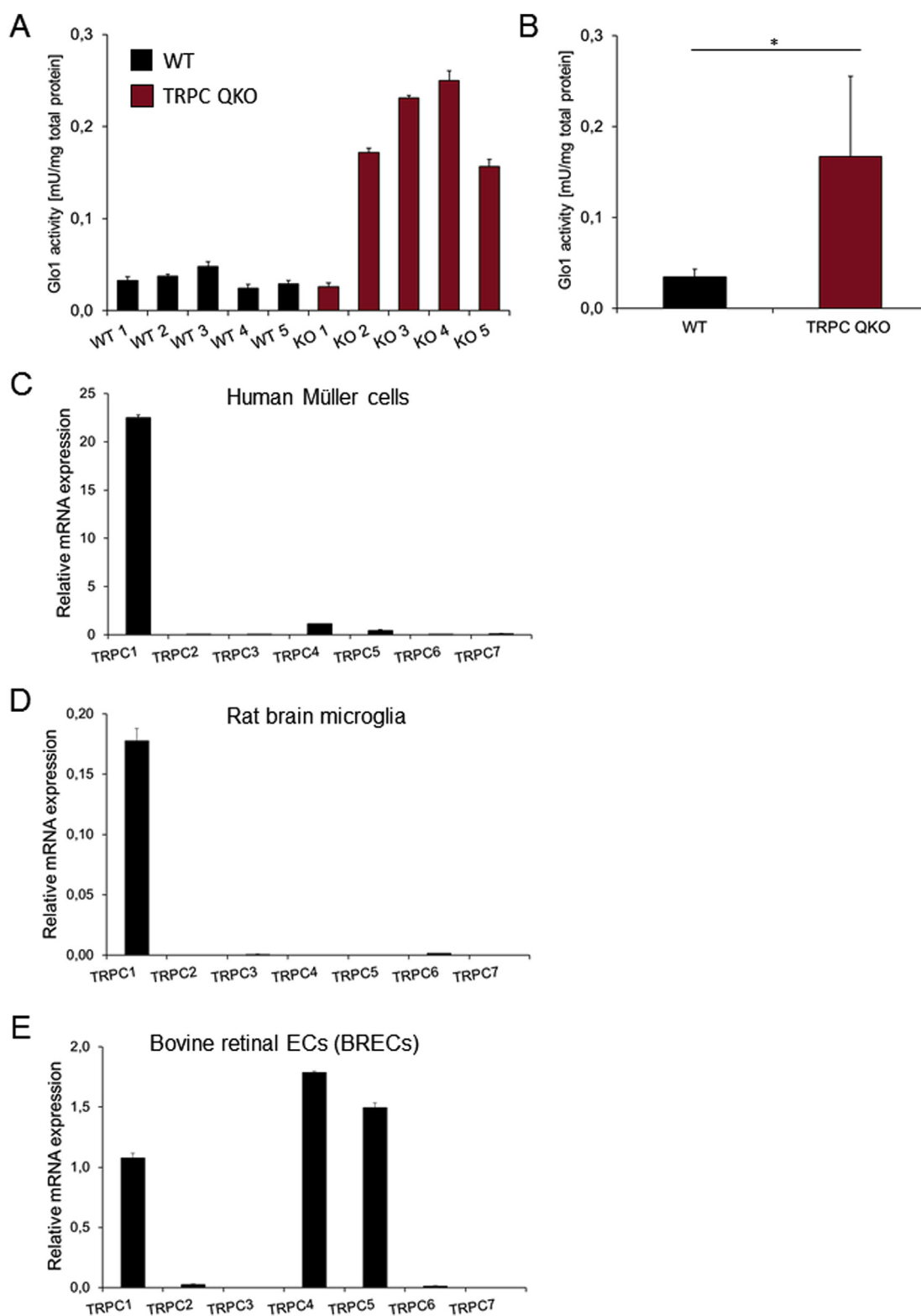


**Figure 6: Increased Glyoxalase 1 activity in the retinæ of *Trpc1/4/5/6*<sup>-/-</sup> mice.** (A) The retinæ were lysed by sonication, and cytoplasmic extracts were used to determine GLO1 activity and normalized to the total protein content in the cytoplasmic extracts. GLO1 activity for retinal extracts of five individual wild-type (WT1-5) and *Trpc1/4/5/6*<sup>-/-</sup> mice (KO1-5) is displayed (\**p* < 0.05). (B) Average GLO1 activity of the 5 wild-type and 5 *Trpc1/4/5/6*<sup>-/-</sup> retinæ (\**p* < 0.05) displayed in (a). (C) Relative mRNA expression levels determined by quantitative real-time PCR (qPCR) analysis of *Trpc* transcripts in RNA samples derived from human Müller cells (*n* = 1). (D) Relative expression levels of *Trpc* transcripts in RNA samples determined in primary rat brain microglia cells (*n* = 1). (E) Relative expression levels of *Trpc* transcripts in RNA samples determined in bovine retinal endothelial cells (BRECs) (*n* = 15).

accumulation. TRPC5 activation was also shown to occur by interaction with oxidized glutathione (GSSG), which rises intracellularly upon MG accumulation [50]. GSSG was shown to activate TRPC5-containing channels via S-glutathionylation [16] and thus, Ca<sup>2+</sup>-dependent cellular processes including cell death are triggered. Increased levels of the TRPC5 modulator GSSG can be evoked upon long-term exposure to MG [50,51]. MG accumulation under diabetic conditions leads to a decrease in endothelial cell number in vessels of mice with STZ-induced diabetes. Interestingly, EC death was prevented in mice overexpressing GLO1 [52], and GLO1 activity was shown to depend on TRPC channels in our study. In addition to the reactive metabolites mentioned before, a plethora of other agonists able to trigger TRPC channel activity could be envisaged under diabetic conditions as underlying mechanisms to initiate cellular processes and cell death in endothelial or other retinal cells. Despite various possible mechanisms discussed above, the identification of the exact trigger events underlying TRPC channel-mediated damage to the neurovascular unit will be subject for further investigations.

An emerging question for future studies will be to find the functional link between the presence of TRPC proteins and GLO1-mediated MG detoxification. Our data in TRPC deficient cells show an increase of GLO1 protein expression in MEF cells and in the retina homogenates, suggesting that TRPC function limits GLO1 protein expression and thereby GLO1 enzyme activity as well as MG detoxification. TRPC channels could mediate calcium-dependent gene expression via calcium-dependent transcription factors such as members of the NFAT family [53]. However, calcium-dependent suppression of genes would be rather an exception. Alternatively, TRPC function could modulate post-translational modification of GLO1 proteins. Recently, it was reported that a transient rise in cytosolic calcium levels results in more persistent ubiquitination of proteins [54,55]. If GLO1 proteins were also ubiquitylated in a Ca<sup>2+</sup>-dependent manner, it would be conceivable that proteasome-targeting of the ubiquitinated GLO1 proteins and their degradation is reduced in TRPC-deficient cells. Finally, TRPC-mediated calcium entry could modulate GLO1 enzyme activity, but a variation of the calcium concentration across a wide range between 100 nmol/L to 3 μmol/L did not affect GLO1 enzyme activity in our experiments (data not shown). To corroborate that the increase in GLO1 expression and activity were responsible for the increased protection against MG in TRPC QKO cells, GLO1 antagonists could be used to see whether the improved viability in TRPC QKO MEF cells can be shifted to the range observed in WT cells. However, application of the GLO1 inhibitor S-p-bromogluthathione cyclopentyl diester (BBGC) [56,57] per se evoked considerable (>50%) cell death in MEF cells in concentrations needed for efficient enzyme inhibition (>5 μM, data not shown), hampering the significance of such an approach. Alternatively, the increase in GLO1 expression and enzyme activity does not necessarily denote whether GLO1-independent mechanism(s) also contribute to detoxification of MG or other reactive metabolites in the absence of TRPC1/4/5/6. Indeed, we have observed alternative pathways in cells, in which GLO1 expression and enzyme activity were abolished following GLO1 gene deletion in Schwann cells; here, we found up-regulation of genes encoding aldo-keto reductases (AKR) as well as an increase in AKR enzyme activity [58]. However, we found upregulation of AKR activity only when GLO1 was completely abolished, and the key enzymes of metabolic pathways that might be upregulated in TRPC QKO cells need to be identified as to causally address the relevance of such pathways.

Pharmacological inhibition of TRPC channels could be an attractive future approach for the treatment of DR. Several TRPC blockers have been described, but there are constraints for in vivo application.

Recently, an inhibitor of TRPC4- and TRPC5-homomeric channels as well TRPC1/TRPC4- and TRPC1/TRPC5-heteromeric channels has been developed [59]. This blocker (compound C31 or pico145) has been shown to be highly potent (IC<sub>50</sub> in the range of 5–1300 pM) and specific within the TRP channel family. However, its effectiveness in primary cells and in vivo has not yet been demonstrated. Apart from C31, there are other TRPC channel blockers available such as SAR7334 and ML204. SAR7334 blocks TRPC3, TRPC7, and, most potently, TRPC6 homomeric channels [60]. ML204 was identified as a TRPC4 and TRPC5 inhibitor. However, its pharmacokinetic properties limit its use in vivo [61]. SAR7334 application abolished hypoxia-induced increases in pulmonary arterial pressure in a similar way as observed in *Trpc6*<sup>-/-</sup> mice.

Taken together, in this study, we demonstrate a causal contribution of TRPC proteins for the development of diabetic retinopathy in the murine STZ model and provide evidence that TRPC-mediated processes aggravating vasoregression as well as neurodegeneration in the retina may be due to a TRPC-mediated role in the accumulation of the reactive metabolite MG and its detoxification by GLO1. However, in future studies, the exact TRPC-containing channel entities and the cell type(s) that initiate(s) TRPC-dependent processes in DR need to be identified to understand the causative role of TRPCs in DR precisely.

## FUNDING

This work was supported by several grants including SFB 1118 (“Reactive Metabolites as cause of diabetic long-term complications”) to MF, HPH, TF, PN, and the INTERNATIONAL RESEARCH TRAINING GROUP 1874/1 (Diabetic Microvascular Complications, DIAMICOM) and the Intramural Research Program of the NIH (project ZO1-ES-101684 to LB).

## CONFLICT OF INTEREST

The authors confirm no conflict of interest associated with this manuscript

## CONTRIBUTION STATEMENT

R.S., A.S., D.S., C.M., N.D., U.K., and T.F. carried out experiments. R.S., A.S., D.S., C.M., N.D., U.K., T.F., I.M., R.M., P.N. H.P.H., and M.F. analyzed and interpreted data. P.N., H.P.H., and M.F. provided research support. MF conceived and designed the study. R.S., D.S., and M.F. wrote the paper. T.F., P.N., and H.P.H. revised the paper.

## ACKNOWLEDGEMENT

We thank Hans-Peter Gensheimer and Yoko Oguchi for technical assistance.

## APPENDIX A. SUPPLEMENTARY DATA

Supplementary data related to this article can be found at <https://doi.org/10.1016/j.molmet.2018.01.003>.

## REFERENCES

- [1] Forbes, J.M., Cooper, M.E., 2013. Mechanisms of diabetic complications. *Physiological Reviews* 93:137–188.
- [2] Giacco, F., Brownlee, M., 2010. Oxidative stress and diabetic complications. *Circulation Research* 107:1058–1070.

- [3] Bierhaus, A., Fleming, T., Stoyanov, S., Leffler, A., Babes, A., Neacsu, C., et al., 2012. Methylglyoxal modification of Nav1.8 facilitates nociceptive neuron firing and causes hyperalgesia in diabetic neuropathy. *Nature Medicine* 18:926–933.
- [4] Eberhardt, M.J., Filipovic, M.R., Leffler, A., de la Roche, J., Kistner, K., Fischer, M.J., et al., 2012. Methylglyoxal activates nociceptors through transient receptor potential channel A1 (TRPA1): a possible mechanism of metabolic neuropathies. *Journal of Biological Chemistry* 287:28291–28306.
- [5] Andersson, D.A., Gentry, C., Light, E., Vastani, N., Vallortigara, J., Bierhaus, A., et al., 2013. Methylglyoxal evokes pain by stimulating TRPA1. *PLoS One* 8: e77986.
- [6] Song, M.Y., Makino, A., Yuan, J.X., 2011. Role of reactive oxygen species and redox in regulating the function of transient receptor potential channels. *Antioxidants and Redox Signaling* 15:1549–1565.
- [7] Miller, B.A., Zhang, W., 2011. TRP channels as mediators of oxidative stress. *Advances in Experimental Medicine and Biology* 704:531–544.
- [8] Hofmann, T., Schaefer, M., Schultz, G., Gudermann, T., 2002. Subunit composition of mammalian transient receptor potential channels in living cells. *Proceedings of the National Academy of Sciences USA* 99:7461–7466.
- [9] Goel, M., Sinkins, W.G., Schilling, W.P., 2002. Selective association of TRPC channel subunits in rat brain synaptosomes. *Journal of Biological Chemistry* 277:48303–48310.
- [10] Broker-Lai, J., Kollwe, A., Schindeldecker, B., Pohle, J., Nguyen Chi, V., Mathar, I., et al., 2017. Heteromeric channels formed by TRPC1, TRPC4 and TRPC5 define hippocampal synaptic transmission and working memory. *The EMBO Journal* 36:2770–2789.
- [11] Strubing, C., Krapivinsky, G., Krapivinsky, L., Clapham, D.E., 2003. Formation of novel TRPC channels by complex subunit interactions in embryonic brain. *Journal of Biological Chemistry* 278:39014–39019.
- [12] Montell, C., Birnbaumer, L., Flockerzi, V., 2002. The TRP channels, a remarkably functional family. *Cell* 108:595–598.
- [13] Wu, L.J., Sweet, T.B., Clapham, D.E., 2010. International Union of Basic and Clinical Pharmacology. LXXVI. Current progress in the mammalian TRP ion channel family. *Pharmacological Reviews* 62:381–404.
- [14] Yoshida, T., Inoue, R., Morii, T., Takahashi, N., Yamamoto, S., Hara, Y., et al., 2006. Nitric oxide activates TRP channels by cysteine S-nitrosylation. *Nature Chemical Biology* 2:596–607.
- [15] Xu, S.Z., Sukumar, P., Zeng, F., Li, J., Jairaman, A., English, A., et al., 2008. TRPC channel activation by extracellular thioredoxin. *Nature* 451:69–72.
- [16] Hong, C., Seo, H., Kwak, M., Jeon, J., Jang, J., Jeong, E.M., et al., 2015. Increased TRPC5 glutathionylation contributes to striatal neuron loss in Huntington's disease. *Brain: A Journal of Neurology* 138:3030–3047.
- [17] Ma, R., Chaudhari, S., Li, W., 2016. Canonical transient receptor potential 6 channel: a new target of reactive oxygen species in renal physiology and pathology. *Antioxidants and Redox Signaling* 25:732–748.
- [18] Poteser, M., Graziani, A., Rosker, C., Eder, P., Derler, I., Kahr, H., et al., 2006. TRPC3 and TRPC4 associate to form a redox-sensitive cation channel. Evidence for expression of native TRPC3-TRPC4 heteromeric channels in endothelial cells. *Journal of Biological Chemistry* 281:13588–13595.
- [19] Graham, S., Yuan, J.P., Ma, R., 2012. Canonical transient receptor potential channels in diabetes. *Experimental Biology and Medicine* 237:111–118.
- [20] Stitt, A.W., Curtis, T.M., Chen, M., Medina, R.J., McKay, G.J., Jenkins, A., et al., 2016. The progress in understanding and treatment of diabetic retinopathy. *Progress in Retinal and Eye Research* 51:156–186.
- [21] Kolibabka, M., Friedrichs, P., Dietrich, N., Fleming, T., Schlotterer, A., Hammes, H.P., 2016. Dicarbonyl stress mimics diabetic neurovascular damage in the retina. *Experimental and Clinical Endocrinology & Diabetes: Official Journal, German Society of Endocrinology [and] German Diabetes Association* 124:437–439.
- [22] Wang, J., Takeuchi, T., Tanaka, S., Kubo, S.K., Kayo, T., Lu, D., et al., 1999. A mutation in the insulin 2 gene induces diabetes with severe pancreatic beta-cell dysfunction in the Mody mouse. *Journal of Clinical Investigation* 103:27–37.
- [23] Dietrich, A., Kalwa, H., Storch, U., Mederos y Schnitzler, M., Salanova, B., Pinkenburg, O., et al., 2007. Pressure-induced and store-operated cation influx in vascular smooth muscle cells is independent of TRPC1. *Pflügers Archiv: European Journal of Physiology* 455:465–477.
- [24] Freichel, M., Suh, S.H., Pfeifer, A., Schweig, U., Trost, C., Weissgerber, P., et al., 2001. Lack of an endothelial store-operated Ca<sup>2+</sup> current impairs agonist-dependent vasorelaxation in TRPA<sup>-/-</sup> mice. *Nature Cell Biology* 3: 121–127.
- [25] Xue, T., Do, M.T., Riccio, A., Jiang, Z., Hsieh, J., Wang, H.C., et al., 2011. Melanopsin signaling in mammalian iris and retina. *Nature* 479:67–73.
- [26] Dietrich, A., Mederos, Y.S.M., Gollasch, M., Gross, V., Storch, U., Dubrovskaya, G., et al., 2005. Increased vascular smooth muscle contractility in TRPC6<sup>-/-</sup> mice. *Molecular and Cellular Biology* 25:6980–6989.
- [27] Wajcman, H., 2003. Analysis of hemoglobins and globin chains by high-performance liquid chromatography. *Methods in Molecular Medicine* 82: 21–29.
- [28] Geiss, G.K., Bumgarner, R.E., Birditt, B., Dahl, T., Dowidar, N., Dunaway, D.L., et al., 2008. Direct multiplexed measurement of gene expression with color-coded probe pairs. *Nature Biotechnology* 26:317–325.
- [29] Dietrich, N., Hammes, H.P., 2012. Retinal digest preparation: a method to study diabetic retinopathy. *Methods in Molecular Biology* 933:291–302.
- [30] Dietrich, N., Kolibabka, M., Busch, S., Bugert, P., Kaiser, U., Lin, J., et al., 2016. The DPP4 inhibitor linagliptin protects from experimental diabetic retinopathy. *PLoS One* 11:e0167853.
- [31] McLellan, A.C., Phillips, S.A., Thornalley, P.J., 1992. The assay of methylglyoxal in biological systems by derivatization with 1,2-diamino-4,5-dimethoxybenzene. *Analytical Biochemistry* 206:17–23.
- [32] McLellan, A.C., Thornalley, P.J., 1989. Glyoxalase activity in human red blood cells fractionated by age. *Mechanism of Ageing and Development* 48:63–71.
- [33] Freichel, M., Kriebs, U., Vogt, D., Mannebach, S., Weissgerber, P., 2011. Strategies and protocols to generate mouse models with targeted mutations to analyze TRP channel functions. In: Zhu, M.X. (Ed.), *TRP channels*, Boca Raton (FL).
- [34] McVicar, C.M., Ward, M., Colhoun, L.M., Guduric-Fuchs, J., Bierhaus, A., Fleming, T., et al., 2015. Role of the receptor for advanced glycation end-products (RAGE) in retinal vasodegenerative pathology during diabetes in mice. *Diabetologia* 58:1129–1137.
- [35] Tiruppathi, C., Freichel, M., Vogel, S.M., Paria, B.C., Mehta, D., Flockerzi, V., et al., 2002. Impairment of store-operated Ca<sup>2+</sup> entry in TRPC4<sup>(-/-)</sup> mice interferes with increase in lung microvascular permeability. *Circulation Research* 91:70–76.
- [36] Sundivakkam, P.C., Freichel, M., Singh, V., Yuan, J.P., Vogel, S.M., Flockerzi, V., et al., 2012. The Ca(2+) sensor stromal interaction molecule 1 (STIM1) is necessary and sufficient for the store-operated Ca(2+) entry function of transient receptor potential canonical (TRPC) 1 and 4 channels in endothelial cells. *Molecular Pharmacology* 81:510–526.
- [37] Di, A., Mehta, D., Malik, A.B., 2016. ROS-activated calcium signaling mechanisms regulating endothelial barrier function. *Cell Calcium* 60:163–171.
- [38] Yue, Z., Xie, J., Yu, A.S., Stock, J., Du, J., Yue, L., 2015. Role of TRP channels in the cardiovascular system. *American Journal of Physiology Heart and Circulatory Physiology* 308:H157–H182.
- [39] Orrenius, S., Zhivotovsky, B., Nicotera, P., 2003. Regulation of cell death: the calcium-apoptosis link. *Nature Reviews Molecular Cell Biology* 4:552–565.
- [40] Eder, P., Molkentin, J.D., 2011. TRPC channels as effectors of cardiac hypertrophy. *Circulation Research* 108:265–272.
- [41] Kaczmarek, J.S., Riccio, A., Clapham, D.E., 2012. Calpain cleaves and activates the TRPC5 channel to participate in semaphorin 3A-induced neuronal growth cone collapse. *Proceedings of the National Academy of Sciences USA* 109:7888–7892.

- [42] Puro, D.G., 2007. Physiology and pathobiology of the pericyte-containing retinal microvasculature: new developments. *Microcirculation* 14:1–10.
- [43] Burdyla, T., Borysova, L., 2014. Calcium signaling in pericytes. *Journal of Vascular Research* 51:190–199.
- [44] Earley, S., Brayden, J.E., 2015. Transient receptor potential channels in the vasculature. *Physiological Reviews* 95:645–690.
- [45] Verkhratsky, A., Reyes, R.C., Parpura, V., 2014. TRP channels coordinate ion signaling in astroglia. *Reviews of Physiology, Biochemistry and Pharmacology* 166:1–22.
- [46] Lee, K.P., Yuan, J.P., Hong, J.H., So, I., Worley, P.F., Muallem, S., 2010. An endoplasmic reticulum/plasma membrane junction: STIM1/Orai1/TRPCs. *FEBS Letters* 584:2022–2027.
- [47] Bhardwaj, R., Hediger, M.A., Demaurex, N., 2016. Redox modulation of STIM-ORAI signaling. *Cell Calcium* 60:142–152.
- [48] Prakriya, M., Lewis, R.S., 2015. Store-Operated calcium channels. *Physiological Reviews* 95:1383–1436.
- [49] Li, Z., Guo, G., Wang, H., Si, X., Zhou, G., Xiong, Y., et al., 2017. TRPC5 channel modulates endothelial cells senescence. *European Journal of Pharmacology* 802:27–35.
- [50] Jiang, B., Le, L., Liu, H., Xu, L., He, C., Hu, K., et al., 2016. Marein protects against methylglyoxal-induced apoptosis by activating the AMPK pathway in PC12 cells. *Free Radical Research* 50:1173–1187.
- [51] Wu, L., Juurlink, B.H., 2002. Increased methylglyoxal and oxidative stress in hypertensive rat vascular smooth muscle cells. *Hypertension* 39:809–814.
- [52] Vulesevic, B., McNeill, B., Giacco, F., Maeda, K., Blackburn, N.J., Brownlee, M., et al., 2016. Methylglyoxal-induced endothelial cell loss and inflammation contribute to the development of diabetic cardiomyopathy. *Diabetes* 65:1699–1713.
- [53] Camacho Londono, J.E., Tian, Q., Hammer, K., Schroder, L., Camacho Londono, J., Reil, J.C., et al., 2015. A background Ca<sup>2+</sup> entry pathway mediated by TRPC1/TRPC4 is critical for development of pathological cardiac remodelling. *European Heart Journal* 36:2257–2266.
- [54] Mukherjee, R., Das, A., Chakrabarti, S., Chakrabarti, O., 2017. Calcium dependent regulation of protein ubiquitination - interplay between E3 ligases and calcium binding proteins. *Biochimica et Biophysica Acta* 1864:1227–1235.
- [55] McGourty, C.A., Akopian, D., Walsh, C., Gorur, A., Werner, A., Schekman, R., et al., 2016. Regulation of the CUL3 ubiquitin ligase by a calcium-dependent Co-adaptor. *Cell* 167:525–538 e514.
- [56] Vince, R., Daluge, S., Wadd, W.B., 1971. Studies on the inhibition of glyoxalase I by S-substituted glutathiones. *Journal of Medicinal Chemistry* 14:402–404.
- [57] Thornalley, P.J., Ladan, M.J., Ridgway, S.J., Kang, Y., 1996. Antitumor activity of S-(p-bromobenzyl)glutathione diesters in vitro: a structure-activity study. *Journal of Medicinal Chemistry* 39:3409–3411.
- [58] Morgenstern, J., Fleming, T., Schumacher, D., Eckstein, V., Freichel, M., Herzig, S., et al., 2017. Loss of glyoxalase 1 induces compensatory mechanism to achieve dicarbonyl detoxification in mammalian Schwann cells. *Journal of Biological Chemistry* 292:3224–3238.
- [59] Rubaiy, H.N., Ludlow, M.J., Henrot, M., Gaunt, H.J., Miteva, K., Cheung, S.Y., et al., 2017. Picomolar, selective, and subtype-specific small-molecule inhibition of TRPC1/4/5 channels. *Journal of Biological Chemistry* 292:8158–8173.
- [60] Maier, T., Follmann, M., Hessler, G., Kleemann, H.W., Hachtel, S., Fuchs, B., et al., 2015. Discovery and pharmacological characterization of a novel potent inhibitor of diacylglycerol-sensitive TRPC cation channels. *British Journal of Pharmacology* 172:3650–3660.
- [61] Freichel, M., Tsvilovskyy, V., Camacho-Londono, J.E., 2014. TRPC4- and TRPC4-containing channels. *Handbook of Experimental Pharmacology* 222: 85–128.